Lateral Mechanical Coupling of Stereocilia in Cochlear Hair Bundles

Matthias G. Langer,* Stefan Fink,* Assen Koitschev,† Ulrich Rexhausen,‡ J. K. Heinrich Hörber,§ and J. Peter Ruppersberg‡

*Division of Sensory Biophysics, Hals-Nasen-Ohren Klinik, and Departments of †Otorhinolaryngology and ‡Physiology II, Universität Tübingen, 72076 Tübingen, and §European Molecular Biology Laboratory, 69117 Heidelberg, Germany

ABSTRACT For understanding the gating process of transduction channels in the inner ear it is essential to characterize and examine the functional properties of the ultrastructure of stereociliary bundles. There is strong evidence that transduction channels in hair cells are gated by directly pulling at the so-called tip links. In addition to these tip links a second class of filamentous structures was identified in the scanning and transmission electron microscope: the side-to-side links. These links laterally connect stereocilia of the same row of a hair bundle. This study concentrates on mechanical coupling of stereocilia of the tallest row connected by side-to-side links. Atomic Force microscopy (AFM) was used to investigate hair bundles of outer hair cells (OHCs) from postnatal rats (day 4). Although hair bundles of postnatal rats are still immature at day 4 and interconnecting cross-links do not show preferential direction yet, hair bundles of investigated OHCs already showed the characteristic V-shape of mature hair cells. In a first experiment, the stiffness of stereocilia was investigated scanning individual stereocilia with an AFM tip. The spring constant for the excitatory direction was $2.5 \pm 0.6 \times 10^{-3}$ N/m whereas a higher spring constant ($3.1 \pm 1.5 \times 10^{-3}$ N/m) was observed in the inhibitory direction. In a second set of experiments, the force transmission between stereocilia of the tallest row was measured using AFM in combination with a thin glass fiber. This fiber locally displaced a stereocilium while the force laterally transmitted to the neighboring untouched taller stereocilia was measured by AFM. The results show a weak force interaction between tallest stereocilia of postnatal rats. The force exerted to an individual stereocilium declines to 36% at the nearest adjacent stereocilium of the same row not touched with the fiber. It is suggested that the amount of force transmitted from a taller stereocilium to an adjacent one of the same row depends on the orientation of links. Maximum force transmission is expected to appear along the axis of interconnecting side links. In our studies it is suggested that transmitted forces are small because connecting side links are oriented very close to an angle of 90° with respect of the scan direction (excitatory-inhibitory direction).

INTRODUCTION

The cochlea is the organ of hearing of the mammalian inner ear, transducing sound into an electrical signal. It imbeds the organ of Corti with the mechanosensitive structures known as the hair cells. The organ is located on the top of the basilar membrane showing a characteristic vibration pattern when being stimulated by incoming sound (Von Békésy, 1960). The organ of Corti contains two types of sensory cells: one row of inner hair cells (IHCs) and three rows of outer hair cells (OHCs). A receptive organelle, composed of so-called stereocilia, is located on top of these cells. The stereocilia differ in length at different positions along the mammalian cochlea, reflecting the influence of frequency, and are organized in specific patterns, depending on the function of the particular cell population (Furness et al., 1989; Furness and Hackney, 1985; Russell and Richardson, 1987; Lim, 1986; Zine and Romand, 1996). In this study we concentrate on hair bundles of OHCs arranged in a typical V- or W-like pattern. The cilia within a single row are the same height, whereas stereocilia of different rows are graded in height, the outermost row being the tallest. Adjacent stereocilia of a hair bundle are connected to one another with fine filaments called links. Depending on their geometric arrangement, filaments are divided into two classes: the side and the tip links (Pickles et al., 1984). Besides the cross-links the stereocilia cytoskeleton plays an important role for the elastic properties of hair bundles. The cytoskeleton of stereocilia consists of a dense arrangement of parallel oriented actin filaments forming a core and a root embedded in a platform made of actin on top of the cell, called the cuticular plate (Tilney and Tilney, 1986). At the base the number of actin filaments is reduced from a few hundred to about a dozen, forming a point of flexing. The actin filaments are cross-linked by smaller filaments, probably fimbrin, preventing bending of stereocilia along their length. This construction allows stereocilia to flex around their pivot point located at the bottom where actin filaments penetrate the cuticular plate. A fibrous layer, called tectorial membrane, overlies the organ of Corti, contacting the tips of the tallest stereocilia of the OHCs. The origin of stereocilia displacement is a relative displacement between the basilar and the tectorial membrane forming together with the hair cells a layered or sheet-like structure. In a great number of experiments (Zhao et al., 1996; Marquis and Hudspeth, 1997) it was shown that the presence and orientation of links are directly related to the sensory function of hair cells. A force exerted along the major axis of the stereociliary bundle toward the tallest row of stereocilia (excitatory direction) results in a relative displacement between neigh-

Received for publication 20 June 2000 and in final form 1 March 2001.

Address reprint requests to Dr. Matthias G. Langer, Division of Sensory Biophysics, Hals-Nasen-Ohren Klinik, Universität Tübingen, Röntgenweg 11, 72076 Tübingen, Germany. Tel.: 49-7071-298-7452; Fax: 49-7071-22917; E-mail: matthias.langer@uni-tuebingen.de.

0006-3495/01/06/2608/14 $2.00

boring taller and shorter stereocilia. The tip links, connecting the tips of shorter stereocilia to the lateral wall of adjacent taller stereocilia, are supposed to work like an elastic spring pulling directly at the mechanosensory transduction channels. Opening of the transduction channels results in an influx of cations into the hair cell (Gillespie, 1995; Markin and Hudspeth, 1995). The transduction channels were found to be located in the apical region of stereocilia (Jaramillo and Hudspeth, 1991; Denk et al., 1995). Here, we concentrate on the second population of links, the side links. These links laterally connect the stereocilia of the same row. The function of these links is not well understood yet, but up to now they are thought to tightly connect the entire hair bundle (Howard and Ashmore, 1986). The ultrastructure of sensory hair bundles of the mammalian inner ear has been extensively studied by scanning and transmission electron microscopy (SEM and TEM) (Pickles et al., 1984; Lenoir et al., 1987; Russell and Richardson, 1987). These methods are restricted to fixed and dehydrated specimens, however. For studying the biophysical properties of living hair cells, methods such as patch clamp and small force probes have been applied to isolated and cultured hair cells. Hudspeth and Corey (1977) could show for bullfrog hair cells that movement of the stereocilia toward the kinocilium (excitatory direction) causes a depolarization whereas movement in the opposite direction (inhibitory direction) leads to a hyperpolarization of the hair cell. Howard and Hudspeth (1988) later developed the hypothesis of the gating spring, an elastic element, by which the force is generated to open the transduction channel. Since then, linear and nonlinear force-deflection relations of stereocilia have been a central topic in mechanotransduction research. Over the past 23 years numerous micromechanical measurements have been conducted on entire stereocilia bundles of inner ear sensory hair cells. Most of the data have been acquired from bullfrog saccular hair cells differing in their morphology from the mammalian cochlear hair cells. Stiffness measurements of stereocilia have been conducted by coupling various types of probes to entire stereocilia bundles or by studying Brownian motion of stereocilia by laser interferometry (Howard and Ashmore, 1986; Howard and Hudspeth, 1988; Crawford and Fettiplace, 1985; Strelioff and Flock, 1984; Géléoc et al., 1997; Russell et al., 1992). They showed for sacculus hair cells of the frog and cochlear hair cells of the turtle that stereocilia pivot about their points of insertion and that applied forces are shared almost equally among all stereocilia. Howard and Hudspeth (1988) demonstrated for sacculus hair bundles of the frog that the gating springs contribute to half of the bundle's stiffness, which was confirmed by Russell et al. (1992) for hair bundles from OHCs of postnatal mice. Moreover, Crawford and Fettiplace (1985) found that step displacements of the fixed end of the flexible fiber caused the hair cell's membrane potential to execute damped oscillations with frequencies ranging from 20 to 320 Hz for different cells. They conclude that turtle cochlear hair cells contain an active force-generating mechanism. Direct mechanical stimulation of OHCs from the mouse (Géléoc et al., 1997) with a water jet allowed an estimation of the maximum number of channels: 82 in OHCs, corresponding to about one transducer channel per tip link. In contrast to this result, Denk et al. (1995) observed in bullfrog hair cells transduction channels at both ends of tip links. However, micromechanical experiments on the level of individual stereocilia have not been possible with these techniques. Even if it would be possible to mechanically stimulate an individual stereocilium, it would be still unclear whether adjacent stereocilia in the same row were also pulled via side-to-side links. This would limit the detection of an individual transduction channel to very small stimuli. The possibility of studying the kinetics of a single transduction channel over the whole range of its open probability therefore depends on the strength of cross-linking of stereocilia. Considering the mechanical effect of lateral links on hair bundle elasticity the following situations are conceivable. 1) The hair bundle mechanically behaves as a single unit. Lateral links connecting adjacent stereocilia have approximately infinite stiffness, being much higher than that of an individual stereocilium. 2) When displacing an individual stereocilium, only the nearest neighbors are displaced, too. Stiffness of lateral links is in the range of stiffness of an individual stereocilium. 3) Each stereocilium moves independently from its neighbors. The effect of lateral links on movement of adjacent stereocilia is negligible.

These three working hypotheses were tested by conducting atomic force microscopy (AFM) measurements on the level of individual stereocilia. AFM was used as a point-like probe for displacement of individual stereocilia of OHCs from juvenile rats and examination of the network of cross-links (Langer et al., 2000). AFM was chosen for studying the elastic properties of stereocilia because it has already been applied with success in bioscience to analyze either structural (Binnig et al., 1986) or micromechanical and viscoelastic surface properties of biological samples. Specimens such as the surface of membrane patches (Hörber et al., 1992), the cell surface of MDCK monolayers (Hoh and Schoenenberger, 1994), human platelets (Radmacher et al., 1996), and cultured rat atrial myocytes (Shroff et al., 1995) were examined. Two different types of experiments have been performed to investigate the effect of lateral links on the local elasticity of hair bundles and on force transmission between adjacent stereocilia. In the first one, individual stereocilia of an OHC have been deflected with the AFM tip allowing us to calculate the stiffness as a function of stereocilium position within the hair bundle. In a second experiment, force transmission between adjacent tallest stereocilia was directly measured stimulating one to two stereocilia with a fine glass probe while scanning the entire hair bundle with an AFM tip.

MATERIALS AND METHODS

Sample preparation

Organs of Corti were isolated from 4-day-old rats (Wistar, Interfauna, Germany) according to the method used by Sobkowicz et al. (1975) and Russell and Richardson (1987) for mice. They were cut into three sections (basal, medial, and apical) and placed with the basilar membrane onto Cell-TAK-coated (Becton Dickinson, Heidelberg, Germany) glass coverslips with a diameter of 10 mm. The sample was transferred into Ø 35-mm Falcon dishes filled with 3 ml of culture medium (MEM D-VAL (Gibco BRL Life Technologies, Paisley, UK) with 10% heat-inactivated fetal calf serum and 10 mM HEPES buffer, pH 7.2) supplemented at 310 K and 5% CO_2. Using this preparation, hair bundles of OHCs are oriented perpendicular to the surface of the supporting glass coverslip. For experiments, specimens were transferred from the incubator to a specimen chamber. Cochlear cultures were bathed at room temperature (295 K) in a solution containing (in mM): 144 NaCl, 0.7 NaH_2PO_4, 5.8 KCl, 1.3 $CaCl_2$, 0.9 $MgCl_2$, 5.6 D-glucose, 10 HEPES-NaOH, pH 7.4, osmolarity 304 mOsmol. The solution was exchanged before and after investigation using a conventional perfusion system to keep cells in good condition. Four to six days after birth the tectorial membrane of rats shows different states in length. In a small number of preparations, the tectorial membrane directly touched the hair bundles of OHCs. In those cases, the membrane was removed with a cleaning pipette under the light microscope allowing free access of the AFM tip from the top. Cultures were investigated for a maximum of 2 h.

Experimental setup

All experiments were conducted with a custom-made AFM setup (Langer et al., 1997) combined with an upright light microscope and two additional micro-manipulators. The light microscope (Axioskop FS I, Zeiss, Oberkochen Germany) uses infrared differential interference contrast (DIC) and an Achroplan 40×/0.75 water immersion objective (Zeiss) providing information from a thin optical plane of thick biological specimens (50–250 μm) such as the organ of Corti. The combination of an AFM with such optics is essential for precise vertical approach of the AFM tip to the top of hair bundles, which are ~1.5–2.0 μm in length. A piezoelectric stack (type pa/qna/10/8 × 8; Marco, Hermsdorf, Germany) allows vertical fine positioning (maximum range, 20 μm) of the specimen chamber. Vertical position of the chamber is adjusted by changing the voltage at the piezoelectric stack with a potentiometer. A two-axis translation stage (stage M-461-XY-M; Newport, Darmstadt, Germany) allows horizontal coarse positioning of the specimen chamber in two dimensions. Force interaction between AFM tip and specimen is detected using a slightly modified optical deflection method (Meyer and Amer, 1988; Langer et al., 1997). The AFM detector signal was low-pass filtered using an eight-pole Bessel filter (NPI Electronic, Tamm, Germany) with a cutoff frequency of 10 kHz. V-shaped Si_3N_4 microlevers with a pyramidal shaped tip (typical radius of curvature, 50 nm; tip angle, 70°) and a spring constant of 1×10^{-2} N/m were used (ThermoMicroscopes, Sunnyvale, CA). The AFM tip is scanned with a piezoelectric tube (material VP-A55, Ø 10.2 mm; length, 25.4 mm; Valpey Fisher Corp., Hopkinton, MA). The outer electrode is segmented into eight commensurate electrodes electrically connected in a way that the walls at the end of the piezoelectric tube remain perpendicular to the direction of motion (Siegel et al., 1995). The AFM tip consequently moves on a plane surface in contrast to piezoelectric tube scanners with only four outer electrodes scanning on a curved surface. The software program Pulse++ 1.7 (developed by Ulrich Rexhausen, Institute of Physiology II, Tübingen, Germany, and Klaus Bauer, Max Planck Institute for Medical Research, Heidelberg, Germany) allows the definition of voltage patterns driving the piezoelectric scanner. This program is specially designed for electrophysiological and AFM applications based on Power Macintosh computers (Apple Computer, Cupertino, CA) and an 8-channel 16-bit analog-digital/digital-analog converter board ITC 16 (Instrutech Corp., Great Neck, NY). A triangular-shaped signal was defined in the Pulse++ editor as a fast driving signal for the piezoelectric scanner and converted to an analog voltage signal by the ITC-16 board. Five percent of the top and the bottom of the triangular signal was replaced by a parabolic function. This reduces higher harmonics in the frequency spectrum possibly exciting oscillations of the AFM scanner at its resonance frequency (1.9 kHz). A second analog output of the board was connected to the piezoelectric tube scanner for slow step-like movements of the AFM sensor from scan line to scan line. It is possible to generate up to four independent time-correlated voltage signals, giving the opportunity to simultaneously drive four different devices of the experimental setup. The Pulse++ software additionally allows recording up to four signals at the same time at a maximum bandwidth of 25 kHz. Sampling rate for all experiments was 24 μs/point. Our AFM is equipped with two micromanipulators: a hydraulic-driven 3-axis translation device (Narashige Scientific Instrument Laboratories, Tokyo, Japan) and a micrometer screw-driven 3-axis manipulator (stage M-461-XYZ-M, Newport). The hydraulic manipulator supports positioning of cleaning pipettes (tip diameter, 5–15 μm) in the range of 10 × 10 × 10 mm, whereas the screw-driven manipulator was used for coarse positioning of glass fibers with small tips (tip diameter, 229 ± 21 nm (mean ± SD)). Cleaning pipettes were fabricated of 2-mm borosilicate glass (Science Products, Hofheim, Germany) using a DMZ universal puller (Zeitz-Instrumente Vertrieb, München, Germany). Fine glass fibers were fabricated of 1-mm borosilicate glass (Science Products) using a laser puller (model P-2000, Sutter Instrument Co., Novato, CA). These fibers were used for accurately defined displacement of stereocilia but not for exerting a certain force to the hair bundle. Buckling and bending of fibers was kept to a minimum adjusting the parameters of the laser puller such that the tips reveal a conical shape. For control, the bending stiffness of the fiber was measured by applying a force perpendicular to the fiber axis with a calibrated AFM cantilever. The bending stiffness of those fibers was in the range from 5.0×10^{-1} to 6.5×10^{-1} N/m being ~20 times stiffer than investigated stereocilia. For displacement of stereocilia the fiber was moved in axial direction and not at a right angle to the fiber axis, supposing a much higher stiffness for this direction of stimulation. For experiments they were attached to a piezoelectric tube (material VP-A55, 10.2 mm; length, 25.4 mm; Valpey Fisher Corp.) allowing axial positioning and modulation with nanometer precision. In this paper means are given ±SD.

Experimental procedure

For all experiments the spring constant of cantilevers was calibrated using a method reported by Cleveland et al. (1993). An additional mass was attached to the free moving end, shifting the resonance frequency of a cantilever to lower frequencies. The spring constant of the cantilever is a direct function of the frequency shift. Glass spheres of 10 μm in diameter (Duke Scientific Corp., Palo Alto, CA) were used as a loading mass. Mass was calculated by multiplying the volume of the sphere $((4/3)\pi(\text{diameter}/2)^3)$ by the density (2.42 g/cm^3) of the glass sphere. Spheres were picked up with a cleaning glass pipette (see above) and attached to the top of the hollow AFM tip.

Spring constants for the longest triangular-shaped cantilever varied from 0.75×10^{-2} to 1.30×10^{-2} N/m. All AFM investigations were performed in the constant-height mode switching off the feedback electronics. The relative angle between the scan direction and the specimen support was measured by taking line scans by AFM on the flat glass coverslip at the bottom of the chamber. Both directions were aligned parallel using the slope correction of the AFM electronics.

Stiffness measurement

Due to the orientation of hair cells in the organ of Corti, the stiffness was horizontally measured in direction of the AFM tip motion whereas in most AFM experiments the stiffness is generally measured perpendicular to the

scan plane (Weisenhorn et al., 1989; Burnham et al., 1990). First, the direction of AFM tip motion and axis of symmetry of the OHC bundles were adapted by adjusting the specimen chamber. For approaching the cantilever a hair bundle of interest was visually selected in the light microscope and directly positioned below the AFM tip by adjusting the specimen stage. A piezoelectric stack allows vertical fine positioning of the specimen chamber while scanning the AFM cantilever tip (scan range, 4.5 μm). The AFM tip was horizontally scanned at a right angle to the triangular-shaped cantilever beam. The approach was stopped as soon as the stereocilia of the OHCs caused significant deflection of the Si_3N_4 cantilever (~20–50 nm). The detector signal was monitored on a digital storage oscilloscope (HM 1007, Hameg, Frankfurt/Main, Germany) and a computer display. For stiffness measurements the AFM tip scanned each stereocilium of a hair bundle. During the scan only the tallest stereocilia of the hair bundle were touched by the lateral face of the pyramidal tip and deflected in excitatory and inhibitory directions (see Langer et al., 2000). Fig. 1 shows a typical example of an AFM trace. The ordinate displays the vertical deflection of the AFM cantilever while scanning an individual stereocilium. It has been demonstrated (Langer et al., 2000) that the positive slope of the force curve (when in contact with the sample) depends on the elasticity of the investigated sample. An increase in stiffness as a result, for example, of chemical fixation (Fig. 6 in Langer et al., 2000) leads to an increase in positive slope. This increase in slope reflects that for the same horizontal force exerted by an AFM tip, a stiff stereocilium does not horizontally move as much as a soft stereocilium. The horizontal stiffness k_L of a stereocilium can be calculated from the horizontal force F_L exerted by the AFM sensor and the resulting horizontal displacement x using Hook's law for a linear spring:

$$k_L = F_L/x, \tag{1}$$

where F_L is the exerted force in x direction causing a displacement x. In our experiments, the AFM cantilever exerts a horizontal force F_L to the tips of stereocilia resulting in a horizontal deflection of the sample. Assuming that friction is very low, F_L can be calculated from the measured vertical force F_N (Fig. 2 *A*) using:

$$F_L = F_N \tan \alpha = k_{Cant}\, a \tan \alpha, \tag{2}$$

where α is the angle between the lateral face of the pyramidal-shaped AFM tip and the scan direction, a is the vertical deflection of the cantilever beam,

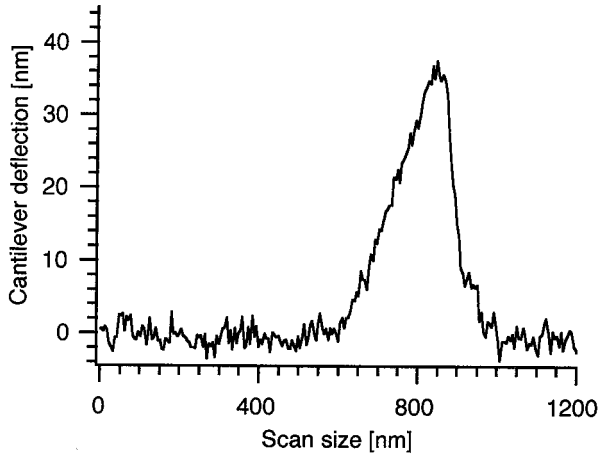

FIGURE 1 Typical AFM trace recorded in excitatory direction on a single stereocilium. The axis of ordinates displays the vertical deflection of the AFM cantilever versus horizontal scan movement of the AFM tip. The scan frequency was 2 Hz. The peak from 600 to ~1000 nm represents the force interaction between AFM tip and stereocilium.

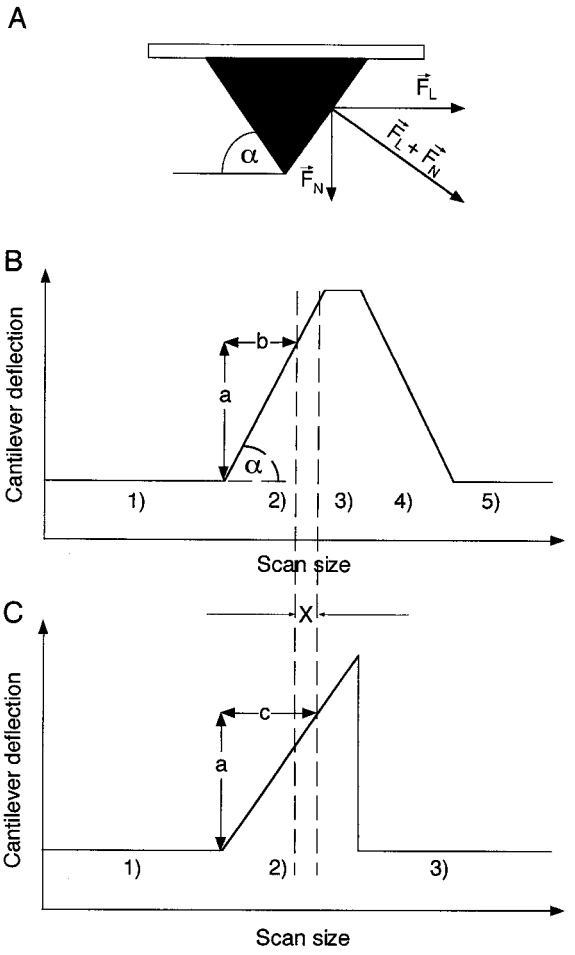

FIGURE 2 Principle of stiffness measurement. (*A*) The horizontal force F_L is calculated from the vertical force F_N according to Eq. 2. The angle α (for our AFM sensors, $\alpha = 55°$) depends on the tip geometry of the AFM probe. The black triangle corresponds to the AFM tip, which is 3 μm in height. The arrows represent the orientation and absolute value of the horizontal force F_L and the detected vertical force F_N. (*B*) Experimental expectation for an AFM scan that was performed on an infinitely stiff pin-like structure. The vertical cantilever deflection is displayed versus horizontal scan movement of the AFM tip. Region 1 corresponds to the situation where the AFM tip does not touch the specimen. At region 2 the cantilever deflection linearly increases. The front plane of the AFM tip touches the stiff object, mapping the lateral plane of the AFM tip. At region 3 the AFM tip scans the flat top of the specimen. Afterwards, it slips down the stiff object thereby imaging the topography of the backside of the AFM tip (region 4). Finally, the AFM tip loses contact and the cantilever is again in its resting position (region 5). The line a indicates the cantilever deflection at a scan size b when in contact with the stiff specimen. (*C*) Experimental expectation for the same AFM scan, but now recorded on an elastic stereocilium. Again, region 1 marks the region of non-contact. At region 2 the tip touches the stereocilium resulting in a nearly linear increase in cantilever deflection. In contrast to the situation displayed in *B* the force exerted by the AFM tip results in a horizontal displacement of the elastic object. At the transition between regions 2 and 3, AFM tip and specimen lose contact. The cantilever nearly instantaneously snaps back to the initial position (beginning of region 3) while the specimen horizontally moves back to the left. The line c indicates the scan range starting from the first point of contact to the point where the cantilever reaches the same vertical deflection a as shown in *B*. The x corresponds to the horizontal displacement of the elastic sample.

and k_{Cant} is the spring constant of the AFM cantilever. For calculating the spring constant k_L in Eq. 1 we still have to assess the horizontal displacement x of the stereocilium. Fig. 2, *B* and *C*, reveal experimental expectations obtained from an infinitely stiff pin-like sample (Fig. 2 *B*) and from an elastic stereocilium (Fig. 2 *C*). The cantilever deflection is displayed versus scan size. b corresponds to the distance between the first point of contact (between AFM tip and stiff sample) and the horizontal position where the AFM tip reaches a vertical deflection a. c represents the distance between the first point of contact (between AFM tip and elastic stereocilium) and the horizontal position where the AFM tip reaches the same vertical deflection a. The horizontal displacement x of an elastic sample (stereocilium) can be calculated subtracting distance b from distance c. This subtraction accounts for the convolution of the tip shape with the measured topography of the sample. The tip shape is defined by the angle α between the scan direction and the lateral face of the tip. Distance b depends on α as follows (Fig. 2 *B*):

$$b = a/\tan\alpha \quad (3)$$

The vertical deflection of the elastic sample is assumed to be negligible for a horizontal displacement x being small compared with the length of the elastic object (stereocilium). Considering these assumptions, we can calculate the force constant k_L, inserting the results of Eqs. 3 and 2 into Eq. 1:

$$k_L = F_L/(c - b) = (k_{Cant}\, a \tan\alpha)/(c - (a/\tan\alpha)) \quad (4)$$

Using the horizontal deflection method described before, it is essential to know the exact angle α between the lateral face of the AFM tip and the scan plane. Therefore, double-beam cantilevers with pyramidal-shaped Si_3N_4 tips having a well-defined tip angle of 70° were used. In contrast to single-beam cantilevers, double-beam cantilevers scanned horizontally at a right angle to the beam direction show only small buckling and torsion at forces smaller than 2 nN. This could be demonstrated (Langer et al., 2000) by scanning a sharp glass tip with a double-beam cantilever at a right angle to the cantilever beam. The resulting angle, calculated from the AFM scan profile, was 53.45°, being close to the expected angle of 55° (angle between pyramidal-shaped tip and scan plane). Results show that horizontal forces in the range up to 2 nN have only little effect on tip orientation and torsion of the cantilever and can therefore be neglected in our experiments. The AFM tip successively scanned each stereocilium of a hair bundle ~10 times. For calculation of the spring constant, the scan line with maximum peak amplitude was chosen. At this particular scan line, the AFM tip is in contact with the center of the stereocilium. Scan lines with smaller peak amplitudes represent a force interaction of the stereocilium with the left or right lateral face (with respect to the scan direction) of the AFM tip. For calculation of the spring constant it was assumed that friction during force interaction is negligible. For control, the investigated hair bundles were scanned a second time adding a sinusoidal modulation signal (peak-to-peak amplitude, 100 nm; frequency, 98 Hz) to the fast scan signal of the piezoelectric tube scanner of the AFM (Göddenhenrich et al., 1994). This results in an additional horizontal forward and backward movement of the AFM tip at higher frequency. When in contact with a stereocilium, the AFM tip moves toward the sample and back, which allows detection of frictional and attractive forces. For negligible friction, the AFM tip slips up and down the identical path while scanning the tip forward and backward at this fast modulation frequency. In the case of frictional forces acting between AFM tip and stereocilium surface, the cantilever movement shows a hysteresis, indicating a slip-stick interaction between tip and sample. Usually, detectable frictional and attractive forces led to loss in spatial resolution in the AFM grayscale image. In those cases it was not possible to detect individual stereocilia in the AFM image (data not shown). For data analysis only those measurements were taken into account where hysteresis of the cantilever movement was not detectable in the AFM signal.

Force transmission measurement

Glass coverslips with attached cochlear cultures were mounted at the bottom of the fluid chamber. Organs of Corti were rotated around their vertical axis until the direction of motion of AFM tip and stimulator were aligned parallel to the axis of symmetry of OHC bundles. Stimulation fibers were attached to a piezoelectric tube actuator mounted on a 3-axis translation stage tilted by 27°. For parallel alignment of fiber and specimen support, the fiber was appropriately angled close to the tip melting the glass capillary with a heated wire. The fiber was coarsely placed under light microscopic control to the axis of symmetry of the OHC bundle using the 3-axis translation stage (Fig. 3 *A*). The

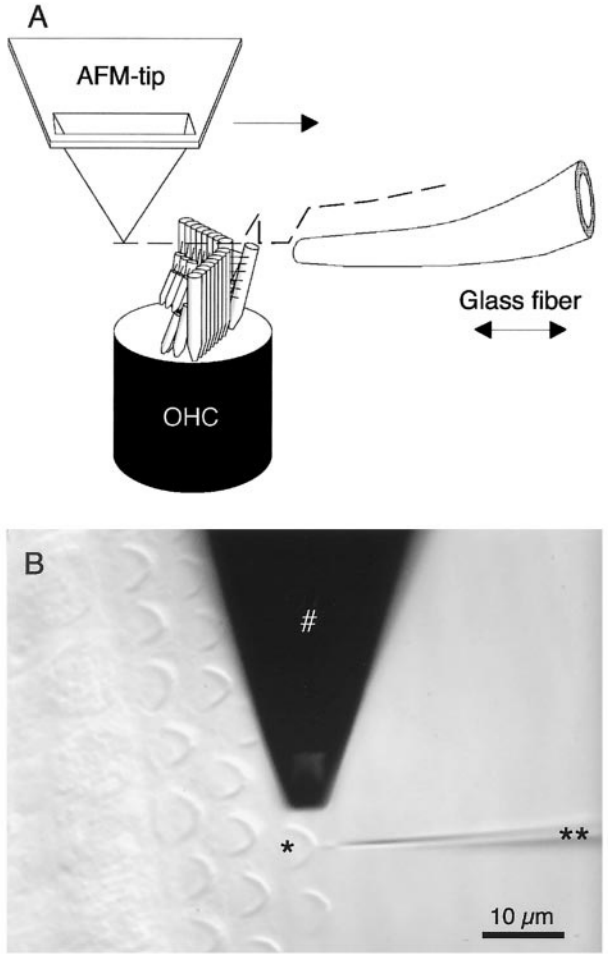

FIGURE 3 Arrangement of OHC bundle, AFM tip, and stimulation fiber for force transmission measurements. (*A*) For local mechanical displacement of a V-shaped hair bundle a glass fiber is approached to a single stereocilium of the tallest row of stereocilia of an OHC. This approach is controlled recording AFM line scans on the glass fiber tip and the hair bundle. The dashed line represents the vertical deflection of the AFM cantilever while scanning from the left to the right. Arrows indicate the scan direction of the AFM cantilever and the direction of stimulation of the glass fiber during force transmission measurements. As indicated in the drawing, force interaction between AFM tip and stereocilium results in a horizontal displacement of the scanned stereocilium. (*B*) Coarse approach of the glass fiber (**) toward the hair bundle (*) was controlled in the light microscope. In contrast to *A* this video image displays the experimental situation from the top. All hair bundles reveal the typical V-shape of outer hair cells. The AFM cantilever (#) is approached from the top to the major axis of the hair bundle.

voltage at the piezoelectric stack of the specimen chamber was adjusted for vertical fine positioning of the hair bundle. For horizontal approach of the stimulating fiber the piezoelectric tube was axially elongated until the fiber tip touched the top of the stereocilium. Relative arrangement of fiber, AFM cantilever, and OHC bundle during the approach is shown in Fig. 3 *B*. Vertical and horizontal fine positioning of fiber and stereocilium were controlled by AFM. The AFM tip scans the upper edge of the fiber tip and the top of a stereocilium during the approach. The resulting AFM detector signal was controlled on the live display of the Pulse++ software program (Fig. 4). After stopping the AFM scan, the fiber was sinusoidally modulated at 357 Hz with an amplitude (peak-to-peak) of 22 nm perpendicular to the axis of the stereocilium. The piezoelectric tube allowing precise modulation of the fiber was driven by a synthesized function generator (SRS Stanford Research Systems, model DS 345, Sunnyvale, CA). The AFM tip was adjusted in height until interaction with the top of the hair bundle led to a vertical cantilever deflection of ~20–50 nm. Two hundred line scans were recorded on the entire hair bundle with the AFM while one to two stereocilia were horizontally modulated with the fiber. Total scan range was 4×4 μm. An AFM scan in the excitatory direction results in a stereocilium deflection toward the stimulating fiber, which should in principle stretch the interconnecting side links between the scanned and adjacent stereocilia. Scanning the AFM tip in the inhibitory direction deflects the stereocilia opposite to the stimulating fiber, which might cause a loss in contact between the fiber and the contacted stereocilia. Therefore, only line scans representing a force interaction in the excitatory direction were considered for calculation of the transmitted force. The magnitude of the AFM signal is exclusively detected at the stimulation frequency of 357 Hz using a lock-in amplifier (software program written in IGOR 3.14 Macro language, WaveMetrics, Lake Oswego, OR). We chose a lock-in amplifier for measuring the transmitted force because it provides a quick and easy performance. The transmitted force was simply measured by scanning the whole hair bundle by AFM while a stimulation fiber locally applies a certain force to the stereociliary bundle. After the experiment, AFM data were processed by the software lock-in amplifier and displayed as a grayscale image allowing proper identification of stereocilia location. In principle, the transmitted force could also be measured by deflecting a stereocilium in small steps (steady-state measurement) instead of using a sinusoidal stimulation. We preferred the second method because the experiment can be conducted within a short period of time and the lock-in technique provides a high signal-to-noise ratio. In comparison with a lock-in-based experiment, steady-state measurements require more time for investigating all stereocilia of the entire hair bundle. We first would have to localize the center of a certain stereocilium by scanning the AFM tip and to stop the scan at this point. Then a stimulation fiber would have to deflect a stereocilium of the same hair bundle in small steps while the AFM measures the force at the localized stereocilium. This procedure has to be repeated for each stereocilium of the hair bundle. Compared with our measurements, this kind of experiment requires more time, which is very critical. The sample may drift between two measurements, requiring a proper control of the relative position of contacted stereocilium and stimulation fiber after each stereocilium measurement. The lock-in amplifier allows sensitive detection of the magnitude of the force signal at the frequency of interest (357 Hz) with high signal-to-noise ratio. Frequency components below and above the stimulation frequency ideally do not contribute to the output signal of the lock-in amplifier. The lateral force F_L was calculated for each stereocilium of the investigated hair cells from the output signal of the lock-in amplifier using Eq. 2. The time constant of the low-pass filter could be adjusted only in steps and was set to 5 ms, keeping the modulation frequency of 357 Hz in the amplifier output signal at a minimum. In our measurements we made use only of the magnitude (signal amplitude) and not of the phase between the signal and the lock-in reference signal.

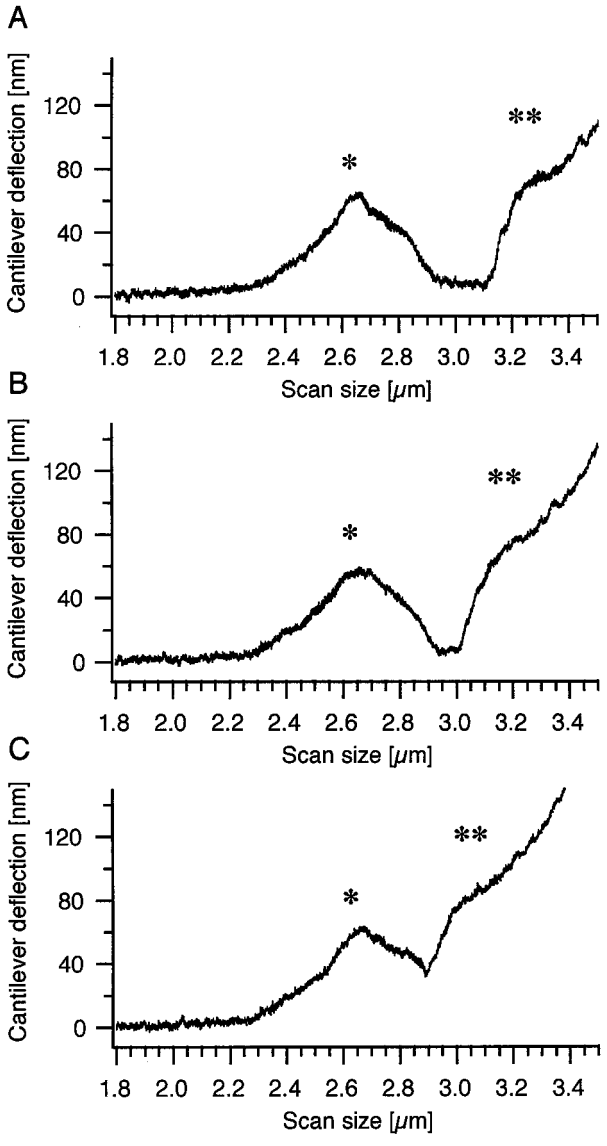

FIGURE 4 AFM line scans recorded at three different times during approach of the glass fiber tip toward a stereocilium. (*A*) AFM trace recorded on an individual stereocilium (*) of an OHC and glass fiber tip (**). (B*)* AFM line scan recorded after shifting the fiber toward the stereocilium. (*C*) AFM trace recorded after the fiber was attached to the stereocilium. The edge of the stimulation fiber touches the tip of the investigated stereocilium.

RESULTS

Stiffness measurement

In a first experiment, stiffness of outer hair bundles (rat P4) was measured at individual stereocilia as a function of stereocilium position within the hair bundle. The trace shown in Fig. 5 *A* represents a typical example of force interaction between the AFM tip and a stereocilium. For determination of the position of a stereocilium within the bundle, the ~200 scan lines recorded on a hair bundle were displayed as a grayscale image revealing the positions of the respective stereocilia tips (see, for example, Fig. 6). The central stereocilium of a hair bundle was defined as 0, and adjacent stereocilia were labeled with numbers starting from

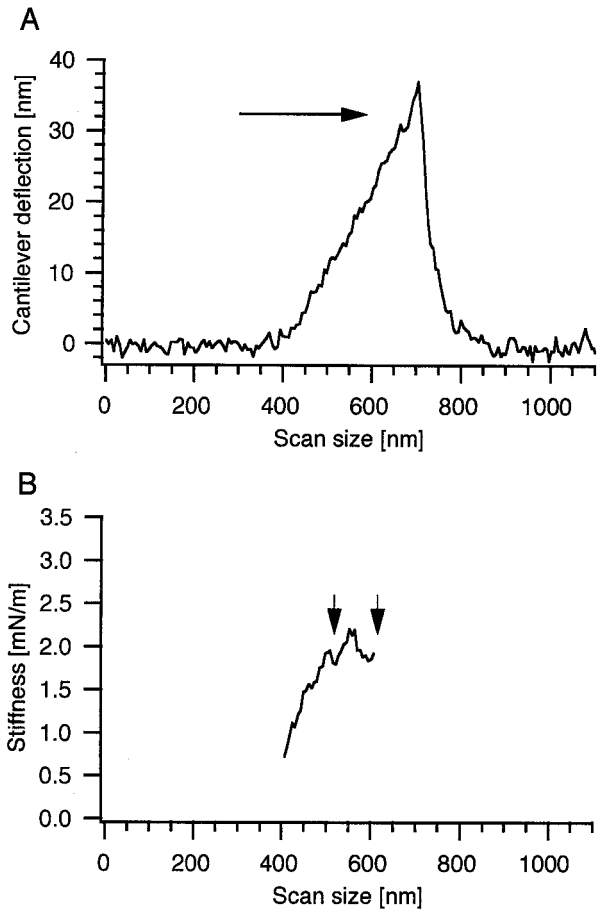

FIGURE 5 Example of an AFM scan recorded on a stereocilium and the corresponding stiffness curve. (*A*) AFM line scan recorded on a stereocilium in excitatory direction. Between 0 and 400 nm the AFM tip is not in contact with the sample. At ~400 nm the cantilever deflection increases nearly linearly, reaching a maximum at ~700 nm. The black arrow indicates the direction of motion of the investigated stereocilium. (*B*) Stiffness (versus scan size) of the stereocilium calculated from the cantilever deflection in *A*. The stiffness was only calculated for that range where the AFM exerts a force to a stereocilium resulting in a horizontal displacement. At a scan size of 400 nm the AFM tip touches the stereocilium for the first time. Mean steady-state stiffness was calculated from data points located between the black arrows.

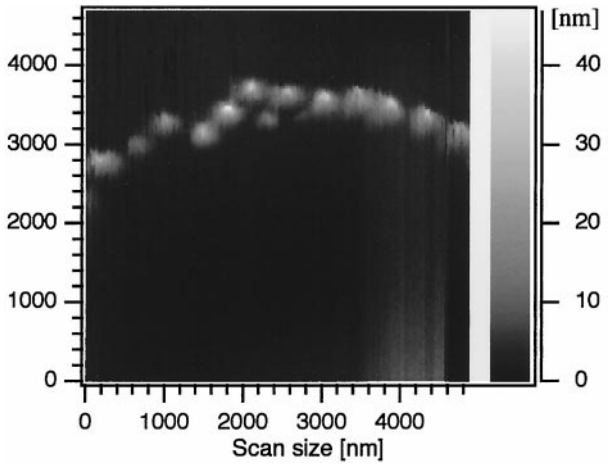

FIGURE 6 AFM image displaying the arrangement of tallest stereocilia of an OHC (rat, postnatal day 4). The tips of the tallest stereocilia appear as white spots standing very close to each other (scan size, 4.87 × 4.7 μm). The grayscale bar encodes the vertical cantilever deflection.

1 for the left half of the hair bundle and −1 for the right half of the hair bundle (as seen in the grayscale image). Hair bundle stiffness as shown in Fig. 5 *B* was calculated according to Eq. 4 from Fig. 5 *A*. Calculation was done only for that range where AFM tip and stereocilium are in contact. Traces shown represent the force interaction in the excitatory direction. The stiffness increases from 0.73×10^{-3} N/m reaching a steady-state level at $\sim 2 \times 10^{-3}$ N/m. For statistics, the mean stiffness has been calculated at the steady-state level. Mean stiffness values of all stereocilia were arranged in a table versus position of the stereocilium in the hair bundle. In Fig. 7, mean stiffness of 17 investigated hair bundles of OHCs (age, P4; basal and medial region) is displayed versus position. Mean stiffness in the excitatory direction is $(2.5 \pm 0.6) \times 10^{-3}$ N/m and in the inhibitory direction is $(3.1 \pm 1.5) \times 10^{-3}$ N/m. Taking into account the standard deviation of 0.6×10^{-3} N/m, the average spring constant (filled squares in Fig. 7 *A*) showed no dependence on the stereocilium position for the excitatory direction. A Student *t*-test was done to test whether there is truly a significant difference between excitatory and inhibitory stiffness. The resulting p value ($p < 0.0001$) confirmed that there is a highly significant difference in stiffness for both directions of stimulation. Although stiffness was measured at individual stereocilia it still needs to be clarified how much adjacent stereocilia contribute to the spring constant. In principle, force exerted by AFM could be transmitted by side links to adjacent stereocilia of the same row and via tip links to adjacent stereocilia of shorter rows. Although the high efficacy of force transmission via tip links has already been demonstrated in numerous micromechanical and electrophysiological studies (Howard and Hudspeth, 1987, 1988; Marquis and Hudspeth, 1997) we still know less about the efficacy of force transmission mediated by side links. This question was directly addressed in a second AFM experiment. Force transmitted between adjacent stereocilia was measured by AFM using a lock-in amplifier in combination with a stimulating glass fiber touching an individual pair of stereocilia.

Force transmission measurement

Line scans recorded on hair bundles of OHCs were displayed as grayscale images (see Fig. 8) allowing an exact localization of stereocilia and the stimulating glass fiber. The force transmitted from the vibrating fiber (position *ii* in Fig. 9 *A*) to the tallest stereocilia of the same hair bundle

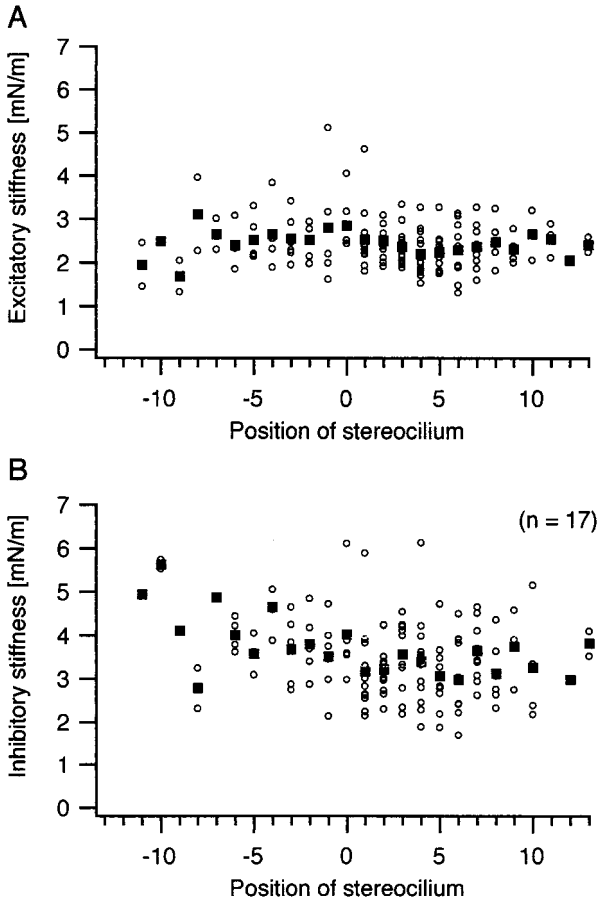

FIGURE 7 Pooled stiffness data of 17 OHCs displayed versus position of stereocilium. Data (OHC age: P4, basal and medial region) are separately displayed for the excitatory (*A*) and inhibitory (*B*) direction. ○, raw data; ■, mean stiffness calculated for all investigated positions within the hair bundle. (*A*) About 97% of all excitatory stiffness values vary from 1.4×10^{-3} to 3.4×10^{-3} N/m. Taking this mean variation into account, no correlation between stiffness and position of stereocilia is visible. (*B*) The same plot as displayed in *A* for the inhibitory direction. Mean variation of stiffness is much bigger compared with the excitatory direction. Stiffness ranges from 1.7×10^{-3} to 6.1×10^{-3} N/m. Mean stiffness (■) seems to slightly increase from position −5 to −10.

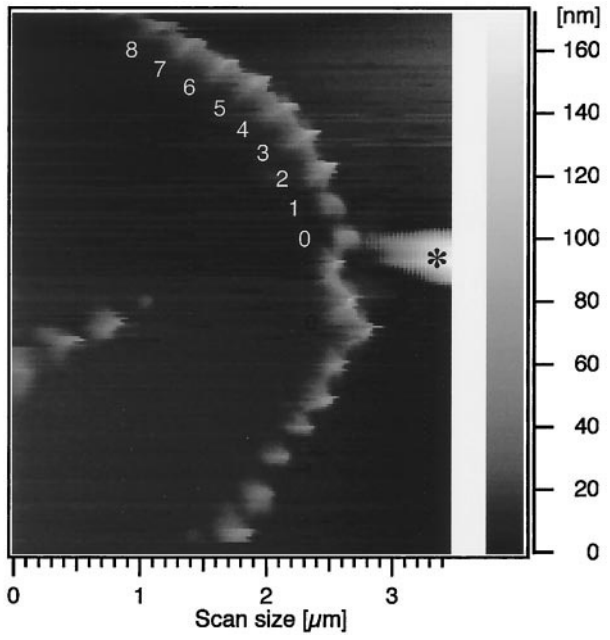

FIGURE 8 AFM grayscale image of an outer hair cell bundle in contact with the stimulating fiber (*). The fiber in contact with a single stereocilium shows a stripe-like pattern, which is due to the periodic movement of the fiber. For stiffness and force plots in Figs. 7, 10, and 11, positions of stereocilia within the hair bundle were labeled with numbers ranging from 0 for the directly contacted up to 8 for the adjacent stereocilia. The scan range is 3.4 × 4.0 μm. The grayscale bar encodes the vertical cantilever deflection; white spots represent the tips of the tallest stereocilia.

could be detected as an oscillation in the AFM signal (position *i* in Fig. 9 *A*) at 357 Hz. For high-resolution detection of the oscillation amplitude the oscillation signal was extracted from the measured AFM signal (Fig. 9 *A*) with the help of a frequency-selective lock-in amplifier. The output of the lock-in amplifier provides the peak amplitude (magnitude) of the 357-Hz oscillation (Fig. 9 *B*). The lateral force F_L transmitted between stereocilia was calculated from the magnitude (time constant was set to 5 ms) using Eq. 2. For each stereocilium the maximum detected force F_L (calculated from the magnitude) was plotted versus stereocilium position (Fig. 10 *A*). A stereocilium or stereocilia in direct contact with the stimulation fiber were labeled as 0, whereas adjacent stereocilia not in direct contact with the fiber were labeled as numbers starting from 1. Only that half of the hair bundle was taken into account, where the fiber was in contact with the directly stimulated stereocilium across its entire width and the nearest adjacent stereocilium was completely untouched by the fiber. The arrangement of stereocilia and stimulating fiber was controlled in the corresponding grayscale image (for example, Fig. 8). Force interaction between stereocilia and AFM tip led to displacements of stereocilia from 0 nm to 249 ± 41 nm. These displacements are expected to be sufficiently high to stretch lateral links interconnecting the directly displaced with adjacent stereocilia of the same row. Measured absolute forces (Fig. 10 *A*) show a fast decline from stereocilium 0 to 1. Variations in maximum detected forces at position 0 are due to differences in pre-load force exerted by the stimulating glass fiber. During the approach of the fiber tip to the stereocilium, the relative position but not the pre-load force was detected. For better comparison of the different measurements shown in Fig. 10 *A*, forces were normalized with respect to the corresponding maximum force detected at the directly stimulated stereocilium. Normalized force in Fig. 10 *B* rapidly decreases from the directly stimulated to the first adjacent stereocilium. Stereocilia located at positions 1–8 reveal only a slight decrease in relative force from 36% to 20%. The normalized force level of ~0.2 still detectable at stereocilia 6–8 located far from the stimulation fiber is

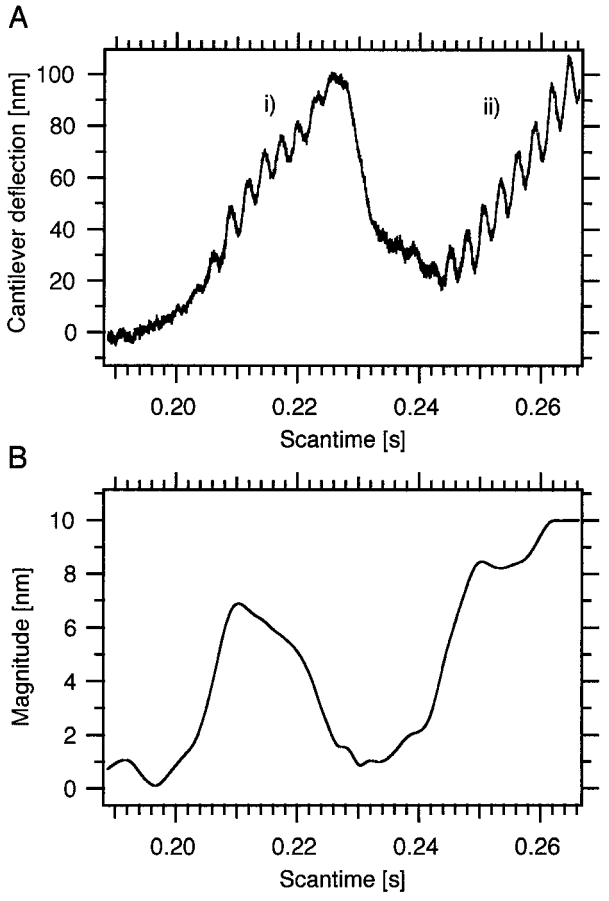

FIGURE 9 Example of an AFM trace and the corresponding magnitude detected at 357 Hz by lock-in. (*A*) Example of an AFM line scan recorded on a stereocilium (*i*) and a vibrating glass fiber (*ii*). The sinusoidal modulation pattern (frequency, 357 Hz) detected at the stereocilium (*i*) is due to the movement of the vibrating glass fiber (*ii*). For calculating the force exerted to the stereocilium, the magnitude of the cantilever vibration at 357 Hz was detected using a lock-in amplifier. (*B*) The output of the lock-in amplifier provides the vertical deflection of the AFM cantilever at 357 Hz containing no phase-related information. This trace shows the resulting magnitude calculated from *A*. As expected, the magnitude of the cantilever vibration is small before contact between AFM tip and stereocilium (from 0.19 to 0.20 s). At ~0.21 s the AFM tip touches the stereocilium, resulting in an increase of the magnitude of the cantilever vibration to ~7 nm. After losing the contact (0.23 s) the magnitude decreases to ~1 nm. While in direct contact with the vibrating glass fiber (from 0.244 to 0.266 s) a maximum magnitude of 10 nm was calculated.

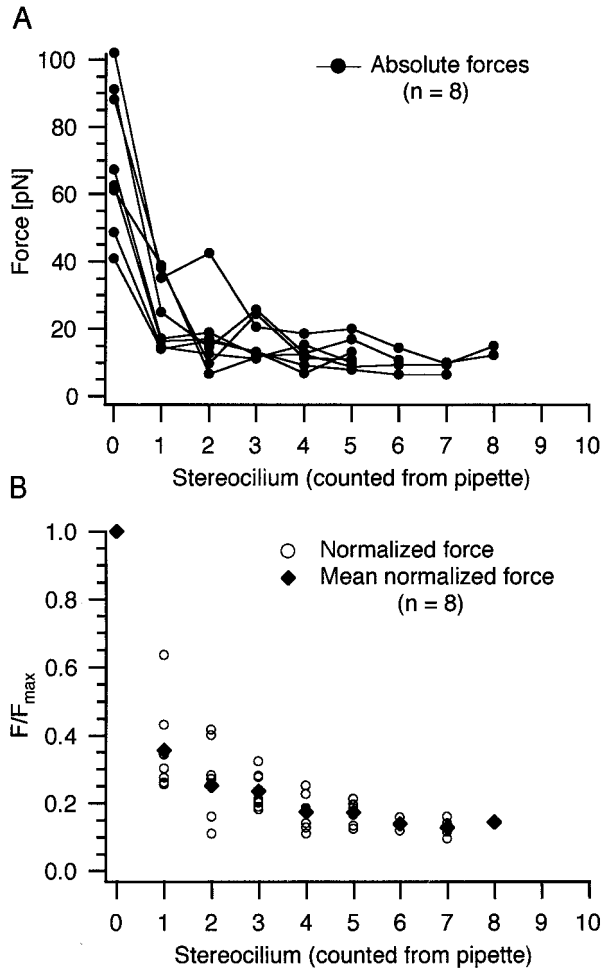

FIGURE 10 Force transmission between adjacent stereocilia of the tallest row of stereocilia. Pooled data of eight hair cell bundles (age: P4, medial region of 2nd and 3rd OHC row) are displayed. At position 0 the fiber touches the stereocilium across its entire diameter whereas adjacent stereocilia are completely untouched. Relative arrangement of fiber and hair bundle was controlled in the AFM image. Adjacent stereocilia not in direct contact with the fiber were labeled as numbers starting from 1. (*A*) Absolute measured horizontal forces are plotted versus stereocilium position. The transmitted lateral force rapidly decreases from the stimulated stereocilium (number 0) to the nearest adjacent stereocilium (number 1). The forces measured for the following adjacent stereocilia (from 2 to 8) show a nearly constant force level around 15 pN. Forces measured at position 0 vary between 40 and 105 pN. For direct comparison, the curves were normalized with regard to the maximum detected force. (*B*) Plot of normalized (○) and mean normalized forces (◆) versus stereocilium position. The transmitted force shows maximum decline between positions 0 and 1. From positions 1–6 the transmitted force declines slightly until a steady state level of ~15% is reached for stereocilia numbers 6–8.

due to the acoustic interference emitted by the piezoelectric actuator driving the stimulation fiber at 357 Hz. This interference appears as small sinusoidal oscillations at 357 Hz in the AFM signal, being independent from forces transmitted by lateral links. These results support the hypothesis of a weak interaction between stereocilia by lateral links. The force level of ~20% for stereocilia located far from the stimulation fiber in Fig. 10 does not allow to distinguish between slight coupling of the tallest stereocilia and the tallest stereocilia only connected by tip links to the adjacent shorter stereocilia. Besides the pure 357-Hz component, AFM traces shown in Fig. 10 also contain information about stereocilia stiffness as described above. We used this information for detecting the mechanical effect of the contacting glass fiber on stiffness of adjacent stereocilia. If lateral links contribute to the stiffness obtained at individual stereocilia,

we would expect to see a higher stiffness for adjacent stereocilia compared with those stereocilia investigated without a fiber (Fig. 7 *A*). Stiffness data were calculated only for the excitatory direction, where the AFM tip displaces the stereocilia toward the fiber tip. The result is shown in Fig. 11. Not only the stiffness (filled circles) of the directly touched stereocilium at position 0 was found to be increased but also the stiffness of stereocilia 1–4. Mean stiffness in the excitatory direction was $(4.8 \pm 1.8) \times 10^{-3}$ N/m. This is ~1.9 times higher compared with the mean stiffness of stereocilia not touched with a fiber. For better comparison, stiffness data shown in Fig. 7 *A* (stereocilia not touched with a fiber) were pasted as open symbols into the same graph. For position 7 the stereocilium with and the stereocilium without a touching glass fiber show approximately identical stiffness. This suggests that on one hand lateral links do not tightly couple adjacent tallest stereocilia of the same row and that small independent movements of single taller stereocilia and their adjacent shorter stereocilia connected by tip links are possible. On the other hand, side links laterally connecting stereocilia transmit a force when sufficiently stretched, and this coupling of stereocilia has similar stiffness as a single displaced stereocilium.

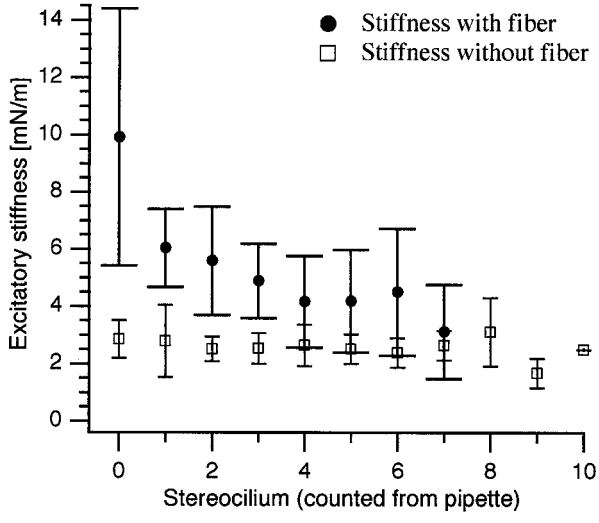

FIGURE 11 Stiffness of stereocilia investigated with and without an attached fiber as a function of position. Before measurements, a fiber was attached to the stereocilium at position 0. Stiffness was measured for the identical hair bundles investigated in Fig. 10. ●, measurements at stereociliary bundles attached to a glass fiber; □, stiffness of stereocilia investigated without a glass fiber (taken from measurements in Fig. 7 *A*). Compared with stereocilia investigated without a supporting fiber, stereocilia located very near to the supporting glass fiber show an increased stiffness. Obviously, interconnection between adjacent stereocilia causes a stiffness increase also at stereocilia not directly contacted by the glass fiber.

DISCUSSION

Stiffness of stereociliary bundles

Taking the standard deviation of 0.6×10^{-3} N/m into account, the average spring constant (filled squares in Fig. 7 *A*) showed no dependence on the stereocilium position for the excitatory direction. In the inhibitory direction, the mean spring constant was slightly higher with a standard deviation being 2.5 times higher compared with the excitatory direction. In the inhibitory direction the taller stereocilia directly touch the adjacent shorter ones whereas in the excitatory direction adjacent shorter stereocilia are pulled by elastic tip links. These links connect the rows of taller and shorter stereocilia (Furness and Hackney, 1985; Lim 1986; Furness et al., 1989; Zine and Romand, 1996). The high standard deviation in the inhibitory direction might be an effect of the variation in spatial interaction between taller and shorter stereocilia. Depending on the angle between scan direction and the direction defined by the centers of adjacent taller and shorter stereocilia, mechanical compliance may vary in a wide range. If we compare our results with hair cell measurements of other scientists (Strelioff and Flock, 1984; Crawford and Fettiplace, 1985; Howard and Ashmore, 1986; Howard and Hudspeth, 1987, 1988; Russell et al., 1992; Géléoc et al., 1997), some methodical differences have to be considered. One major difference is the type of interaction between probe and sample. Whereas most investigators used the probe to deflect the entire hair bundle, we used an AFM tip for local stimulation of individual stereocilia. A brief overview of a selection of publications is shown in Table 1. Compared with mammalian hair bundles, hair bundles from turtles/bullfrogs reveal a somewhat higher stiffness. This could be explained by the different experimental methods used for hair bundle stimulation, the different morphology of stereociliary bundles of species used for investigation, and the degree of maturation. The arrangement of stereocilia of mammalian hair bundles shows a typical V or W shape (Russell and Richardson, 1987; Furness et al., 1989) whereas hair bundles of other vertebrates such as turtle or bullfrog reveal a brush-like conical shape. In mammals the stereocilia directly pick up the mechanical stimulus, whereas in frogs or turtles the kinocilium, connected by cross-links to the stereocilia, acts as an antenna for mechanical stimuli. For frogs and turtles it is therefore essential to have a tight network of cross-links between stereocilia and the kinocilium. Force transmission by lateral links in bullfrog and turtle hair cells has to be efficient. Despite the morphological differences between hair bundles of bullfrogs and rats we can find similarities in the shape of stiffness curves (Fig. 5 *B*) for both species. Stiffness plots presented by Howard and Hudspeth (1988) for hair bundles of the bullfrog sacculus also reveal a minimum at small displacements. The increase in stiffness with increasing displacement of the stereocilia as found by Howard and Hudspeth (1988) corresponds well to our find-

TABLE 1 Calculated stiffness values from various investigators

Type of hair cells	Spring constant 10^{-3} N/m	Rotational stiffness 10^{-15} (N m/rad)	Reference
Turtle (excitatory direction), cochlear hair cells‡ ($l = 6$ μm)	0.59 ± 0.25 ($n = 15$)	22.00†	Crawford and Fettiplace, 1985
Bullfrog (inhibitory + excitatory), saccular hair cells*	0.256 ± 0.028 ($n = 50$)	22.10 ± 2.40†	Howard and Ashmore, 1986
Bullfrog (inhibitory + excitatory), saccular hair cells*	0.93 ± 0.37 ($n = 34$)		Howard and Hudspeth, 1988
Mouse (P1/P2, apical)‡ ($l = 2.6$ μm)			Russell et al., 1992
OHC 3 (inhibitory + excitatory)	1.42 ± 0.38 ($n = 159$)	10.00†	
IHC (inhibitory + excitatory)	1.38 ± 0.32 ($n = 14$)		
Chicken (P3–P7, apical), tall hair cells§ ($l = 6.1 \pm 0.6$ μm)			Szymko et al., 1992
Excitatory direction	0.394 ± 0.184 ($n = 14$)	14.66¶	
Inhibitory direction	0.614 ± 0.306 ($n = 14$)	22.85¶	
Bullfrog (excitatory), saccular hair cells*	0.65 ± 0.31 ($n = 12$)		Jaramillo and Hudspeth, 1993
Mouse cochlea (P1/P2), OHC (inhibitory + excitatory)§ ($l = 4.4 \pm 0.4$ μm)	4.5 ± 1.9 ($n = 8$)	86 ± 37†	Géléoc et al., 1997
Rat cochlea: OHC (P4) ($l = 1.84 \pm 0.20$ μm)			This work
Excitatory direction	2.5 ± 0.6 ($n = 17$)	8.5 ± 3.9	
Inhibitory direction	3.1 ± 1.5 ($n = 17$)	10.5 ± 7.4	

l, length of stereocilia.
*Glass fiber probes were attached to the kinocilium.
†Rotational stiffness given by authors.
‡Glass fiber probes were attached to the top of a stereociliary bundle.
§Hair bundles were stimulated with a water jet.
¶Rotational stiffness calculated from stereocilia length and spring constant given by authors.

ings. Furthermore, Howard and Hudspeth (1988) simultaneously recorded the corresponding receptor potentials, indicating that the transducer was most sensitive over the range of deflection for which the bundle was least stiff. We cannot give a statement about the electrical response of hair cells to an AFM stimulus yet because we still have to measure the transduction current while stimulating individual stereocilia by AFM. Considering the morphology of hair bundles and species, experiments conducted by Russell et al. (1992) and Géléoc et al. (1997) on mouse hair cells fit best to our measurements. Géléoc et al. (1997) used a water jet for stimulation of entire hair bundles. Hair bundle length of 4.4 μm, as given by the authors, is much higher compared with the hair bundles in our investigations. The stiffness in their experiments was calculated from the viscous drag in liquid and the geometry of the bundle modeled as a prolate spheroid. This might explain the stiffness of 4.5×10^{-3} N/m being 1.8 times higher than the stiffness of hair bundles given in this publication. Russell et al. (1992) could show in their experiments for 1–2-day-old-neonatal mice that a glass fiber attached to the top of a V-shaped OHC bundle leads to a saturation of the receptor potential (7 mV) at a hair bundle displacement of 200 nm. We chose a comparable displacement of stereocilia of 249 ± 41 nm to assure that stiffness has been measured for the situation where the maximum receptor potential is expected. In Russell's experiments, steady-state stiffness of 2.60-μm-long hair bundles was 1.42×10^{-3} N/m (Table 1). This is ~1.8 times smaller compared with 2.5×10^{-3} N/m measured in our experiments by AFM for OHCs of postnatal 4-day-old rats. A possible explanation could be the difference in length of hair bundles. For our preparation, SEM studies showed a hair bundle length of 1.84 ± 0.20 μm (calculated from 125 stereocilia). This is ~1.4 times smaller compared with hair bundles investigated by Russell et al. (1992). Taking into account this length, we get a rotational stiffness in the excitatory direction of 8.5 N m/rad, which is close to the rotational stiffness measured by Russell. Experiments conducted by Russell et al. (1992) with a glass fiber showed that attachment of the probe, either to the apex or to the base of the V-shaped bundle of OHCs, made little difference to the stiffness results. This could be explained by a weak interconnection of stereocilia as shown in our measurements in Fig. 10. At both arms of the V-shaped hair bundle, the pipette used in Russell's experiments touched only a small number of stereocilia. Presumably, the glass fiber could displace only the directly contacted stereocilia and their nearest neighbors. Rotational stiffness given in this publication and measured by Russell is smaller by a factor of ~2 compared with the rotational stiffness of turtle and bullfrog stereociliary bundles. This might be due to the different states of maturation of hair bundles. Turtle and bullfrog hair bundles were taken from adult animals whereas in our experiments organs of Corti from young postnatal rats were used. The actin cytoskeleton in stereocilia of postnatal OHCs still develops and tends to become denser at advanced age. For correct interpretation of stereocilia stiffness data the smaller number of actin filaments in postnatal mammalian hair bundles has to be considered.

The mechanical coupling of stereocilia

Force transmission measurements in Fig. 10 reject the hypothesis of strong interaction between adjacent stereocilia

of the tallest row. The strength of tip links could not be controlled in our experiments because the AFM tip scanned only the tallest and not the adjacent stereocilia of shorter rows. In Fig. 10 *A*, absolute forces plotted versus stereocilium position reveal a fast decline from stereocilium 0 directly contacted by the stimulation fiber to the next adjacent stereocilium 1 not contacted by the fiber. There are three possibilities explaining this weak transmission of force: 1) the side links are not intact (broken), 2) the side links between the stereocilia are too weak to transmit the force, or 3) the side links preferentially transmit forces in a certain direction.

A damage of side links due to the removal of the tectorial membrane seems to be unlikely because in most organs of Corti (taken from postnatal rats day 4) used for AFM measurements the tectorial membrane did not directly touch the hair bundles of OHCs. A direct contact between the tectorial membrane and OHC is normally not expected to appear until 6 or 7 days after birth. Nevertheless, the tectorial membrane could contact the hair bundles during the preparation. In this case the fibrous structure of the tectorial membrane as well as the V-shaped arrangement of stereocilia would show a structural disorder. Although the spatial resolution of our light microscope is limited to ~500 nm, morphological artifacts caused by preparation (not used for calculation in this paper) appeared in the microscope as a disorder in the V-shaped hair bundle arrangement. Additionally, the arrangement of stereocilia within a bundle was controlled in the AFM images providing a spatial resolution of better than 1 nm (see Figs. 6 and 8). For control, the arrangement of stereocilia and cross-links of postnatal rats was controlled in the SEM (Langer et al., 2000) after AFM investigation. The hypothesis of a weak interaction was supported by results shown in Fig. 11. Stereocilia being direct neighbors to the stereocilium directly stimulated with a glass fiber showed a significantly higher stiffness compared with those stereocilia of hair bundles investigated without a glass fiber. Measured stiffness of stereocilia decreases rapidly with the distance to the directly stimulated stereocilium. Besides weak force transmission by lateral links, viscoelastic relaxation (e.g., adaptation) of cross-links could be another possible hypothesis explaining the rapid decrease in stiffness and force. In this case one would expect to detect a maximum force at that stereocilium that was investigated first and a decreasing force for stereocilia investigated later. For half of the sets of experiments in Fig. 10, stereocilium 8 was investigated first whereas for the other four sets of experiments measurements were started at stereocilium 0. But no matter which stereocilium was the first one investigated by AFM, stereocilium 0 (directly contacted stereocilium) always showed the maximum force. This indicates that the force measured at different stereocilia of the same hair bundle shows no correlation in time but depends on the stereocilium position. Therefore, it seems to be unlikely that viscoelastic relaxation of the force (via adaptation) has contributed to this decrease in force. Nevertheless, we cannot completely exclude that side links also show adaptation. For verification of adaptation one would have to conduct a different type of experiment as, for example, steady-state measurements, which have already been discussed above. AFM could measure the transmitted force at a certain stereocilium while a glass fiber deflects another stereocilium of the same hair bundle in small steps. In case of adaptation one would expect to see a decrease in stiffness. How can we explain the inconsistency between weak coupling by side links as shown in this publication and tight coupling of stereocilia by tip links (Hudspeth and Markin, 1994)? Tip links are fine molecular threads connecting shorter with adjacent taller stereocilia along the main axis of symmetry. They allow force transmission from a directly displaced taller stereocilium to an adjacent shorter one along the filamentous tip link. In contrast to tip links, side links of cochlear OHCs are oriented at angles ranging from ~45° to 90° with respect to the main axis of symmetry (excitatory-inhibitory direction). This angle depends on the arrangement of stereocilia varying for the three different rows of OHCs in the cochlea. As demonstrated by lock-in measurements, the stimulating glass fiber has only a very local mechanical effect on the nearest adjacent stereocilia. Obviously, the orientation of links in relation to the direction of force exerted to stereocilia plays an important role. Maximum force transmission is expected to appear along the axis of interconnecting side links. In our studies, transmitted force is suggested to be small because side links preferentially transmit forces at a right angle with respect to the AFM stimulus (excitatory-inhibitory direction).

Implications for understanding and further analysis of mechanoelectrical transduction

AFM allows local stiffness measurement on the level of individual stereocilia. Results show that the measured stiffness represents the local elastic properties of the directly contacted stereocilium. Adjacent stereocilia of the same row contribute only slightly. For a partial decoupling of the tectorial membrane from hair bundles of OHCs one might therefore suppose that only stereocilia still in contact with the tectorial membrane and their nearest neighbors are displaced by an incoming mechanical stimulus. Lateral links may not compensate a loss of contact with the tallest stereocilia of OHCs. All results presented in this publication refer to OHCs of postnatal rats at the age of 4 days. During development, the cytoskeleton of stereocilia, the structure of hair bundles, and number of cross-links change (Lenoir et al., 1987; Pickles et al., 1991). It cannot be excluded that the effect of lateral links in adult mammals is different compared with postnatal rats. The length of stereocilia and preferential orientation of links increases with maturation. However, it was shown for postnatal rats that mechanoelectrical transduction is present at day 2 (Kros et al., 1992).

Therefore, we think that for future investigation of the mechanoelectrical transduction in mammals, postnatal rats are appropriate for in vitro assays. Correct interpretation of micro-mechanical data and electrophysiological recordings of transducer currents obtained at hair cells requires exact knowledge of the mechanics of the investigated specimen. Depending on the correlation between force transmission and stereocilium displacement, AFM therefore might be a suitable method for stimulation of only few or individual transduction channels. The number of simultaneously stimulated transduction channels depends on the number of stereocilia connected to the displaced taller stereocilium by tip links. For three rows of stereocilia one would expect an electrical response of two (one channel per tip link) to four channels (one channel at both ends of both tip links). Simultaneous measurements of transducer current amplitude and stiffness on the level of individual stereocilia by patch clamp and AFM will likely further elucidate functional parameters of individual transduction channels and the role of the tip links in their mechano-activation in mammalian hair cells.

We are grateful to Wolfgang Öffner of EMBL Heidelberg for development of the AFM-electronics, Klaus Vollmer of the eye clinic of the University of Tübingen for technical support, and Henry Haase and Petra Rilling for preparation of organs of Corti. We thank Prof. Dr. H. P. Zenner for providing the technical equipment and lab space at the Hearing Research Center in Tübingen and Karsten Löffler for programming the data acquisition software.

This work was supported by the Deutsche Forschungsgemeinschaft (Klinische Forschergruppe Hörforschung DFG Ze 149/6–2 and LA 1227/1–1) and the fortüne program (projects 347–2 and 712–0-0) of the clinics of the University of Tübingen.

REFERENCES

Binnig, G., C. Gerber, and C. F. Quate. 1986. Atomic force microscope. *Phys. Rev. Lett.* 56:930–933.

Burnham, N. A., D. D. Dominguez, R. L. Mowery, and R. J. Colton. 1990. Probing the surface forces of monolayer films with an atomic-force microscope. *Phys. Rev. Lett.* 64:193.

Cleveland, J. P., S. Manne, D. Bocek, and P. K. Hansma. 1993. A nondestructive method for determining the spring constant of cantilevers for scanning force microscopy. *Rev. Sci. Instrum.* 64:403–405.

Crawford, A. C., and R. Fettiplace. 1985. The mechanical properties of ciliar bundles of turtle cochlear hair cells. *J. Physiol.* 364:359–379.

Denk, W., J. R. Holt, G. M. Shepherd, and D. P. Corey. 1995. Calcium imaging of single stereocilia in hair cells: localization of transduction channels at both ends of tip links. *Neuron.* 15:1311–1321.

Furness, D. N., and C. M. Hackney. 1985. Cross links between the stereocilia in the guinea pig cochlea. *Hearing Res.* 18:177–188.

Furness, D. N., G. P. Richardson, and I. J. Russell. 1989. Stereociliary bundle morphology in organotypic cultures of the mouse cochlea. *Hearing Res.* 38:95–109.

Géléoc, G. S. G., G. W. T. Lennan, G. P. Richardson, and C. J. Kros. 1997. A quantitive comparison of mechanoelectrical transduction in vestibular and auditory hair cells of neonatal mice. *Proc. R. Soc. Lond. B.* 264: 611–621.

Gillespie, P. G. 1995. Molecular machinery of auditory and vestibular transduction. *Curr. Opin. Neurobiol.* 5:449–455.

Göddenhenrich, T., S. Müller, and C. Heiden. 1994. A lateral modulation technique for simultaneous friction and topography measurements with the atomic force microscope. *Rev. Sci. Instrum.* 65:2870–2873.

Hoh, J. H., and C. A. Schoenenberger. 1994. Surface morphology and mechanical properties of MDCK monolayers by scanning force microscopy. *J. Cell Sci.* 107:1105–1114.

Hörber, J. K. H., W. Häberle, F. Ohnesorge, G. Binnig, H. G. Liebich, C. P. Czerny, H. Mahnel, and A. Mayr. 1992. Investigation of living cells in the nanometer regime with the scanning force microscope. *Scanning Microsc.* 6:919–930.

Howard, J., and J. F. Ashmore. 1986. Stiffness of sensory hair bundles in the sacculus of the frog. *Hearing Res.* 23:93–104.

Hudspeth, A. J., and D. P. Corey. 1977. Sensitivity, polarity, and conductance change in the response of vertebrate hair cells to controlled mechanical stimuli. *Proc. Natl. Acad. Sci. U.S.A.* 74:2407–2411.

Howard, J., and A. J. Hudspeth. 1987. Mechanical relaxation of the hair bundle mediates adaptation in mechanoelectrical transduction by the bullfrog's saccular hair cell. *Proc. Natl. Acad. Sci. U.S.A.* 84: 3064–3068.

Howard, J., and A. J. Hudspeth. 1988. Compliance of the hair bundle associated with gating of mechanoelectrical transduction channels in the bullfrog's saccular hair cell. *Neuron.* 1:189–199.

Hudspeth, A. J., and V. S. Markin. 1994. The ear's gears: mechanoelectrical transduction by hair cells. *Phys. Today.* 47:22–28.

Jaramillo, F., and A. J. Hudspeth. 1991. Localization of the hair cell's transduction channels at the hair bundle's top by iontophoretic application of a channel blocker. *Neuron.* 7:409–420.

Jaramillo, F., and A. J. Hudspeth. 1993. Displacement-clamp measurement of the forces exerted by gating springs in the hair bundle. *Proc. Natl. Acad. Sci. U.S.A.* 90:1330–1334.

Kros, C. J., A. Rüsch, and G. P. Richardson. 1992. Mechano-electrical transducer currents in hair cells of the cultured neonatal mouse cochlea. *Proc. R. Soc. Lond. B Biol. Sci.* 22:185–193.

Langer, M. G., A. Koitschev, H. Haase, U. Rexhausen, J. K. Hörber, and J. P. Ruppersberg. 2000. Mechanical stimulation of individual stereocilia of living cochlear hair cells by atomic force microscopy. *Ultramicroscopy.* 82:269–278.

Langer, M. G., W. Öffner, H. Wittmann, H. Flösser, H. Schaar, W. Häberle, A. Pralle, J. P. Ruppersberg, and J. K. H. Hörber. 1997. A scanning force microscope for simultaneous force and patch-clamp measurements on living cell tissues. *Rev. Sci. Instrum.* 68:2583–2590.

Lenoir, M., J. L. Puel, and R. Pujol. 1987. Stereocilia and tectorial membrane development in the rat cochlea: a SEM study. *Anat. Embryol.* 175:477–487.

Lim, D. J. 1986. Functional structure of the organ of Corti: a review. *Hearing Res.* 22:117–146.

Markin, V. S. and A. J. Hudspeth. 1995. Gating-spring models of mechanoelectrical transduction by hair cells of the internal ear. *Annu. Rev. Biophys. Biomol. Struct.* 24:59–83.

Marquis, R. E., and A. J. Hudspeth. 1997. Effects of extracellular Ca^{2+} concentration on hair-bundle stiffness and gating-spring integrity in hair cells. *Proc. Natl. Acad. Sci. U.S.A.* 94:11923–11928.

Meyer, G., and N. Amer. 1988. Novel optical approach to atomic force microscopy. *Appl. Phys. Lett.* 53:1054.

Pickles, J. O., S. D. Comis, and M. P. Osborne. 1984. Cross links between stereocilia in the guinea-pig organ of Corti, and their possible relation to sensory transduction. *Hearing Res.* 15:103–112.

Pickles, J. O., M. von Perger, G. W. Rouse, and J. Brix. 1991. The development of links between stereocilia in hair cells of the chick basilar papilla. *Hearing Res.* 54:153–163.

Radmacher, M., M. Fritz, C. M. Kacher, J. P. Cleveland, and P. K. Hansma. 1996. Measuring the viscoelastic properties of human platelets with the atomic force microscope. *Biophys. J.* 70:556–567.

Russell, I. J., M. Kössl, and G. P. Richardson. 1992. Nonlinear mechanical responses of mouse cochlear hair bundles. *Proc. R. Soc. Lond. B.* 250:217–227.

Russell, I. J., and G. P. Richardson. 1987. The morphology and physiology of hair cells in organotypic cultures of the mouse cochlea. *Hearing Res.* 31:9–24.

Shroff, S. G., D. R. Saner, and R. Lal. 1995. Dynamic micromechanical properties of cultured rat atrial myocytes measured by atomic force microscopy. *Am. J. Physiol.* 269:286–292.

Siegel, J., J. Witt, N. Venturi, and S. Field. 1995. Compact large-range cryogenic scanner. *Rev. Sci. Instrum.* 66:2520–2532.

Sobkowicz, H. M., B. Bereman, and J. E. Rose. 1975. Organotypic development of the organ of Corti in culture. *J. Neurocytol.* 4:543–572.

Strelioff, D., and Å. Flock. 1984. Stiffness of sensory-cell hair bundles in the isolated guinea pig cochlea. *Hearing Res.* 15:19–28.

Szymko, Y. M., P. S. Dimitri, and J. C. Saunders. 1992. Stiffness of hair bundles in the chick cochlea. *Hearing Res.* 59:241–249.

Tilney, L. G., and M. S. Tilney. 1986. Functional organization of the cytoskeleton. *Hearing Res.* 22:55–77.

Von Békésy, G. 1960. Experiments in Hearing. MacGraw-Hill, New York.

Weisenhorn, A. L., P. K. Hansma, T. R. Albrecht, and C. F. Quate. 1989. Forces in atomic force microscopy in air and water. *Appl. Phys. Lett.* 54:2651–2635.

Zhao, Y., E. N. Yamoah, and P. G. Gillespie. 1996. Regeneration of broken tip links and restoration of mechanical transduction in hair cells. *Proc. Natl. Acad. Sci. U.S.A.* 24:15469–15474.

Zine, A., and R. Romand. 1996. Development of the auditory receptors of the rat: a SEM study. *Brain Res.* 721:49–58.